Environmental Pollution 405 (2026) 128532

Contents lists available at ScienceDirect

Environmental Pollution

journal homepage: www.elsevier.com/locate/envpol

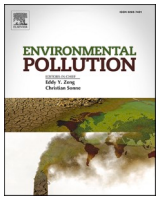

Environmental corona defines the *in vivo* ecotoxicity of polymeric and metal-based nanoparticles in the sea urchin *Paracentrotus lividus*

Patrizia Romano [a,b,*,1], Sofia Bichi [a,1], Nour Oueslati [c], Eugenio Paccagnini [d], Najoua Trigui El Menif [c], Pietro Lupetti [d], Iole Venditti [e], Serena Leone [b], Ilaria Corsi [a]

[a] Department of Physical, Earth and Environmental Sciences, University of Siena, Italy
[b] Department of Biology and Evolution of Marine Organisms (BEOM), Stazione, Zoologica Anton Dohrn, Naples, Italy
[c] Department of Sciences of Bizerte, Laboratory of Environment Biomonitoring, University of Carthage, Zarzouna, Bizerte, Tunisia
[d] Department of Life Sciences, University of Siena, Italy
[e] Department of Sciences, Roma Tre University of Rome, Italy

ARTICLE INFO

Keywords:
Nanoparticles
Eco-corona
Seawater
Echinoderms
Paracentrotus lividus
Oxidative stress
Immune response
Marine ecotoxicology

ABSTRACT

The environmental behavior and biological effects of nanoparticles (NPs) depend strongly on their transformations in seawater and interactions with biotic interfaces. Here, we investigated the physicochemical evolution and ecotoxicological impact of four representative NPs, on the Mediterranean sea urchin *Paracentrotus lividus* under environmentally relevant exposure scenarios. The four type of NPs used are both polymeric amino and carboxylated polystyrene, PS-NH_2 and PS-COOH, and metal-based ones, namely functionalized silver (AgcitLcys) and titanium dioxide (TiO_2). Dynamic light scattering, ζ-potential, and electron microscopy analyses revealed rapid formation of environmental coronas (eco-coronas), arising from the adsorption of natural organic matter, proteins, and dissolved ions present in seawater, and the occurrence of aggregation processes, which varied according to NP core composition and surface charge. *In vivo* exposure assays showed that polymeric NPs induced mild stress responses, while metal-based NPs, characterized by unstable and restructuring coronas, caused marked cytotoxicity, lysosomal destabilization, and activation of immune and antioxidant defenses. Enzymatic biomarkers highlighted tissue-specific oxidative responses, with reduced antioxidant capacity in the sea urchin gonads and the up-regulation of detoxification pathways in the intestine. The integrated use of cellular and enzymatic biomarkers provides mechanistic insights into NPs induced stress responses in marine invertebrates along with eco-corona formation in seawater. As one of the few *in vivo* studies conducted *in vivo* with adults of sea urchins at environmentally relevant exposure concentrations, our findings contribute to bridging the gap between bench-scale studies and realistic exposure scenarios in nanoecotoxicological risk assessment of NPs in marine ecosystems.

1. Introduction

Nanoparticles (NPs) are now embedded in nearly every aspect of modern life, from biomedical applications to consumer products. However, their increasing release into aquatic systems raises pressing questions regarding their environmental fate and biological effects, highlighting the need for robust risk assessment (Turan et al., 2019; Corsi et al., 2020). The marked heterogeneity of NPs, in terms of both core composition and surface functionalization, requires tailored approaches to understand their behaviour and potential effects on aquatic organisms. Once released into marine environments, NPs undergo transformations that profoundly alter their original physicochemical identity, replacing it with a new one shaped by interactions with environmental matrices. This process leads to the formation of the so called environmental corona, or eco-corona, a dynamic layer of biomolecules, including proteins, lipids, polysaccharides, extracellular polymeric substances and humic acids, that spontaneously adsorb onto particle surfaces when in contact with environmental media (*i.e.*, water, sediment/soil, air) (Liu et al., 2022; Yang et al., 2025; Natarajan et al., 2021). This seawater-derived eco-corona should be distinguished from

* Corresponding author. Department of Physical, Earth and Environmental Sciences, University of Siena, Italy.
E-mail address: patrizia.romano@student.unisi.it (P. Romano).
[1] These authors contributed equally to this work.

https://doi.org/10.1016/j.envpol.2026.128532
Received 26 January 2026; Received in revised form 2 June 2026; Accepted 4 June 2026
Available online 10 June 2026

the protein corona that later forms upon interaction with marine organism's biological fluids, such as the coelomic fluid (CF). Depending on both the intrinsic properties of the particles, *i.e.*, size, charge, hydrophobicity, and surface chemistry, and the characteristics of the surrounding medium, such as ionic strength, organic matter, and microbial exudates, the eco-corona may occur either as a loosely associated "soft" layer or as a more stable and persistent "hard" corona (Baalousha et al., 2022). Its formation profoundly affects NP behavior, influencing hydrodynamic size, surface charge, colloidal stability and aggregation, while also defining their biological identity, bioavailability and interactions with cells and organisms (Canesi et al., 2017; Corsi et al., 2020). Among emerging contaminants, particular attention has been devoted to polymeric nanoparticles, such as polystyrene NPs (PS-NPs), which may enter aquatic environments both as by-products of industrial activities and through the progressive fragmentation and degradation of larger plastic debris (Pradel et al., 2023; Permana et al., 2025). Polystyrene is one of the most abundant polymers in plastic litter and can generate nanosized fragments during environmental weathering processes (Besseling et al., 2019; Cole et al., 2011). Carboxylated and aminated polystyrene nanoparticles (PS-COOH and PS-NH_2 NPs) are widely used as models in ecotoxicological studies, as their contrasting surface chemistries provide a standardized platform for investigating the role of surface charge in colloidal behaviour, corona formation, and interactions with marine organisms. Although they should primarily be regarded as experimental proxies, rather than exact replicas of the complexity of environmental nanoplastics, their use is particularly valuable for clarifying the mechanisms through which surface functionalization influences bio-nano interactions and toxicity (Bergami et al., 2017; Grassi et al., 2019; Murano et al., 2021). Beside polymeric NPs, a substantial fraction of nanomaterial pollution arises from metal-based NPs, released through numerous industrial and domestic applications. For instance, silver NPs (AgNPs) are widely used in medical devices, coatings, food packaging, textiles, and water treatment processes for their antimicrobial properties, with an estimated annual global production of ~420-500 tons (Prasher et al., 2020; Jouyban and Rahimpour, 2020; Chatterjee et al., 2022). Their toxicity is attributable both to their nanoscale dimensions and to the release of Ag^+ ions, therefore in recent years we have assisted to the development of eco-safe design approaches to mitigate their environmental impact. One example is the coating with citrate and cysteine (AgcitLcys), conceived to limit ionic release and associated toxicity (Bellingeri et al., 2022). Despite this safer-by-design strategy, AgcitLcys NPs retain the ability to interact with environmental biomolecules and their ecotoxicological effects may depend both on the release, in specific conditions, of Ag^+ ions and on nano-specific interactions with cells, such as membrane adhesion and internalization (Bellingeri et al., 2022, 2024). Titanium dioxide nanoparticles (TiO_2 NPs) are also of major environmental relevance (Keller et al., 2024). Owing to their whitening, UV-blocking, and photocatalytic properties, they are extensively used in cosmetics, sunscreens, food additives, biomedical devices, paints, coatings, and pigments (Gottschalk et al., 2009; Galletti et al., 2016). This versatility has led to their large-scale dissemination and inevitable environmental release, particularly through the daily use of personal care products that directly discharge TiO_2 NPs into coastal waters (Tovar-Sánchez et al., 2013; Zheng et al., 2025). In this context, sensitive species, such as echinoderms, that play key roles in benthic ecosystems, are particularly exposed to NP contamination (Alijagic et al., 2019; Dedman et al., 2021).

The sea urchin *P. lividus* is one of the most widely used models in marine ecotoxicology, owing to its ecological relevance as a benthic keystone species in Mediterranean coastal ecosystems and its economic importance for aquaculture. Its immune cells, the coelomocytes, are extensively used as biosensors of environmental stress (Manzo & Schiavo, 2022; Gambardella et al., 2016; Pinsino and Matranga, 2015). Most of the current knowledge on NPs effects derives from *in vitro* assays and embryotoxicity tests, which have provided valuable insights into cellular and developmental sensitivity (Della Torre et al., 2014; Gambardella et al., 2016). However, these simplified models do not capture the complexity of the interactions occurring between NPs, their eco-coronas, and biological environments, nor the integrated responses that develop within an intact organism. *In vivo* studies on adult *P. lividus* represent a more comprehensive and predictive approach, capable of integrating molecular, cellular, and physiological responses and of assessing NPs fate and toxicity under conditions that closely approximate those of the natural environment. In addition, adult exposure experiments allow for the investigation of key processes such as cellular uptake, immune modulation, oxidative stress, and detoxification across different tissues, providing a realistic view of nano-bio interactions in marine organisms (Alijagic et al., 2019). Despite the potential of this model, *in vivo* studies remain limited, and the effects of eco-corona formation on the physiological responses of sea urchins are still poorly understood. Bridging this gap is essential to achieve a more realistic understanding of NPs environmental behavior and ecotoxicological impact in marine systems.

The present study integrates the physicochemical characterization of eco-corona formation on all four types of NPs (PS-COOH, PS-NH_2, AgcitLcys and TiO_2) in Natural Sea Water (NSW) with *in vivo* experiments on adult *P. lividus* specimens exposed to environmentally relevant and/or predicted concentrations to mimic natural exposure scenarios (Li et al., 2016; Al-Sid-Cheikh et al., 2018; Dedman et al., 2021). A common low-dose exposure level (25 μg L^{-1}), representative of environmentally relevant exposure conditions, was chosen to avoid the use of excessively high concentrations, often adopted in nanoecotoxicological studies. We employed Dynamic Light Scattering (DLS) and Transmission Electron Microscopy (TEM) to unravel the eco-corona formation. Adult *P. lividus* specimens were exposed for 7 days to four type of NPs and their biological responses were assessed through a panel of biomarkers: total red cell count and acetylcholinesterase (AChE) activity in the CF, viability and lysosomal membrane stability (LMS) of coelomocytes, catalase (CAT) activity in the gonads and intestine and glutathione S-transferase (GST) activity in the intestine. By combining eco-corona formation along with NP's colloidal characterization with a multi-biomarker evaluation, this study aims to provide a mechanistic framework for understanding how eco-corona formation influences ecotoxicological responses *in vivo*. This integrated perspective highlights the central role of eco-coronas in modulating NPs behaviour, tissue-specific toxicity, and adaptive responses, thereby advancing the capacity to predict the ecological risks posed by nanomaterials in marine ecosystems.

2. Materials and methods

2.1. Nanoparticle batches

Unlabelled PS-NH_2 (50 nm, positively charged) and PS-COOH (60 nm, negatively charged) NPs were purchased in aqueous dispersion from Bangs Laboratories Inc. (Fishers, IN, USA). TiO_2 NPs (27 ± 2 nm) were provided by Degussa as Aeroxide® P25. AgcitLcys NPs (=8 ± 1 nm, size measured by DLS in Milli-Q using volume-based distribution to better represent primary particles) were prepared according to the procedure described in Prosposito et al. (2019). Prior to each use, NP stock suspensions were sonicated in an ultrasonic bath (Mod. CP316, Ceia; 600 W, 40 kHz, for 3 min) to obtain a homogeneous initial dispersion (Murano et al., 2021).

2.2. Nanoparticle colloidal stability in MilliQ and Natural Sea Water

The colloidal stability of the four NP batches was assessed at a reference concentration of 50 mg L^{-1} in Milli-Q water (Milli-Q) and filtered (0.45 μm) Natural Sea Water (NSW). Immediately before the analysis, NP suspensions were sonicated in an ultrasonic bath (Mod. CP316, Ceia) for 10 s to resuspend the samples. Hydrodynamic diameter (D_H, nm) and ζ-potential (ζP, mV) were measured by dynamic light

scattering (DLS) using a Zetasizer Nano ZS90 (Malvern Instruments) with the Zetasizer software (v.7.02). Measurements were performed at time zero (T_0) in Milli-Q and at T_0, 12 h, and 24 h after incubation in NSW. Transmission electron microscopy (TEM) images of NP dispersions in Milli-Q and NSW after 24 h of incubation were obtained with a Tecnai G2 Spirit (FEI). For TEM, 3 μL of NP suspension were dropped onto Formvar-coated 300 mesh copper grids, blotted after 2 min, and air-dried or negatively stained with 1% uranyl acetate. Particle size analysis was performed by measuring 100 particles with the FIJI ImageJ software. DLS and TEM analyses were also conducted after three PBS washing steps (20 min, 18,000 × g, 18 °C), followed by resuspension in Milli-Q, to characterize NPs with the sole hard corona.

2.3. Animal collection and in vivo nanoparticle exposure

Adult individuals of the Mediterranean sea urchin *P. lividus* (n = 24; average size 7 ± 0.5 cm) were collected in May and October 2024 from the coastal area of Talamone (Grosseto, Tyrrhenian Sea, Italy). Animals were acclimated for 7 days in filtered NSW (0.45 μm; 18 ± 1 °C; salinity 38‰; pH 8) under controlled laboratory conditions and maintained in aquaria with a natural light/dark cycle. After acclimation, 15 individuals in good physiological condition and of comparable size were selected for the *in vivo* exposure experiment. Although sex-related differences in immune and biochemical responses have been reported in *P. lividus*, including coelomocyte-related parameters and antioxidant biomarkers such as catalase and glutathione-related enzymes (Arizza et al., 2013; Marčeta et al., 2020; Asnicar et al., 2024), sex identification was not performed before exposure, as reliable non-invasive protocols were not feasible under the experimental conditions. This represents a limitation of the study and was considered when interpreting the biomarker results. Sea urchins were randomly assigned to five experimental groups: control (NSW only), PS-NH_2, PS-COOH, AgcitLcys, and TiO_2 NPs in NSW at 25 μg L^{-1}, with n = 3 individuals per group. During the exposure period, each sea urchin was maintained individually in a separate beaker under constant aeration, for 7 days with renewal of NP suspensions every 24 h. After 7 days of exposure, animals were immediately dissected at the end of the exposure period, and CF was withdrawn using a 1 mL sterile syringe preloaded with CMFSW-EH anticoagulant solution (1:1, v/v) following Smith's protocol (Smith et al., 2019) and coelomocytes were isolated for viability assay as described below. Gonads and intestine were removed and stored at -80 °C for biochemical and enzymatic analyses. For each experimental group, tissues from the three biological replicates were pooled prior to biochemical and enzymatic assays, and the resulting pooled samples were analyzed in triplicate, in order to obtain a representative treatment-level response and reduce inter-individual variability.

2.4. Immune cells viability

Sea urchin coelomocyte viability was measured according to the protocol of Strober (2015), based on the trypan blue exclusion method. Coelomocytes were isolated from CF by centrifugation at 600 × *g* for 10 min at 4 °C. The cell pellet was resuspended and incubated for 4 min with a 0.4% trypan blue solution prepared in PBS. Stained and unstained cells were then mounted on glass slides and examined under a light microscope (Olympus BX51, Tokyo, Japan). Cell viability was expressed as the percentage of live coelomocytes out of 100 counted.

2.5. Total red cell count

To evaluate the percentage of total red cells (red amoebocytes), 100 μL of coelomocyte suspension in PBS were placed on a slide and incubated for 1 h in a humid chamber at 18 °C in the dark. After removing excess cells, the slides were observed under an optical microscope (40×, Olympus BX51, Tokyo, Japan), and the percentage of red amoebocytes out of 100 immune cells was recorded.

2.6. Lysosomal membrane stability

LMS in coelomocytes was assessed by the neutral red retention time (NRRT) assay, following published protocols (Marques-Santos et al., 2018). Briefly, 200 μL of coelomocyte suspensions obtained by the protocol described above were placed on coverslips (22 × 22 mm) and incubated in a humid chamber at 18 °C for 1 h in the dark. Coelomocytes were then exposed to NR dye solution (40 μg mL^{-1}, prepared from a 40 mg mL^{-1}stock in DMSO) for 30 min, washed with buffer (20 mM HEPES; 436 mM NaCl; 53 mM $MgSO_4$; 12 mM KCl; 12 mM $CaCl_2$; pH 7.5), mounted, and sealed. Slides were examined every 15 min under an optical microscope (40×, Olympus BX51), scoring 100 cells per slide. The endpoint was defined when 50% of cells showed lysosomal leakage. The assay was performed in triplicate and repeated three times.

2.7. Acetylcholinesterase activity

AChE activity was determined in whole CF using the method of Ellman et al. (1961), adapted to a 96-well microplate format. Briefly, each well received 180 μL of reaction buffer (0.1 M NaH_2PO_4, pH 7.2) and 100 μL of CF. The reaction was initiated by adding 10 μL of acetylthiocholine iodide (AThCh, 10 mM). After 15 min of incubation (to allow substrate hydrolysis), 10 μL of DTNB (10 mM) (Ellman's reagent; 2,2′-dinitro-5,5′-dithiobenzoic acid) were added to each well (final volume 300 μL). Absorbance was recorded at 415 nm every 30 s for 5 min using a microplate reader (BIO-RAD, Model 550), and activity was calculated from the linear rate of absorbance increase. For the reagent blank, 300 μL of MilliQ water were added to the well, whereas for the sample blank, 100 μL of CF and 190 μL of reaction buffer were added (without substrate). After 15 min of incubation, 10 μL of DTNB (10 mM) were added to each well. Reaction kinetics were then monitored by measuring absorbance at 415 nm every 30 s for 5 min using a microplate reader (BIO-RAD, Model 550). All measurements were performed in triplicate. Enzyme activity was normalized to CF protein content and expressed as nmol min^{-1} mg $protein^{-1}$.

2.8. Enzymatic and protein assays

Intestines and gonads of *P. lividus* were used for enzymatic analyses. Tissues were placed in a homogenization buffer (50 mM K2HPO4, 0.75 M sucrose, 1 mM EDTA, 0.5 mM DTT, 400 μM PMSF, 10 μM leupeptin, 1 μM pepstatin A, 1 mg/L aprotinin, pH 7.5) at a 1:4 ratio (weight:volume) and centrifuged at 500 × *g* for 15 min at 4 °C, to remove tissue debris and nuclei and the resulting supernatants were centrifuged again at 12,000 × *g* for 30 min to obtain post-mitochondrial fractions. Catalase (CAT, E. C. 1.11.1.6) activity was measured in homogenates from both intestines and gonads by monitoring the decomposition of H_2O_2 at 240 nm and 20 °C, following the kinetic method of Aebi (1984). Glutathione S-transferase (GST, E.C. 2.5.1.18) activity was assessed in intestinal homogenates according to Habig et al. (1974), using CDNB as substrate in the presence of reduced glutathione (GSH). Reactions (220 μl final volume) were performed in black 96-well plates and monitored fluorometrically at 25 °C with excitation at 355 nm and emission at 460 nm using a Victor microplate reader (PerkinElmer). Enzymatic activities were expressed as specific activity in nmol or μmol min^{-1} mg $protein^{-1}$. Protein concentration in the CF and intestine and gonad homogenates was determined using a Bio-Rad protein assay, according to the manufacturer's instructions.

2.9. Statistical analysis

Data were analyzed using the GraphPad Prism software (version X, GraphPad Software, San Diego, CA, USA). Since assumptions of normality and homoscedasticity were not consistently met, non-parametric tests were applied. Differences among experimental groups (control and NP treatments) were evaluated by the Kruskal-Wallis test,

followed by Dunn's multiple comparisons post hoc test. Results were considered statistically significant at $p < 0.05$. Data are presented as mean ± standard deviation (SD).

3. Result and discussion

3.1. Nanoparticles behaviour and eco-corona formation

The colloidal behavior of NPs in NSW is a key determinant of their

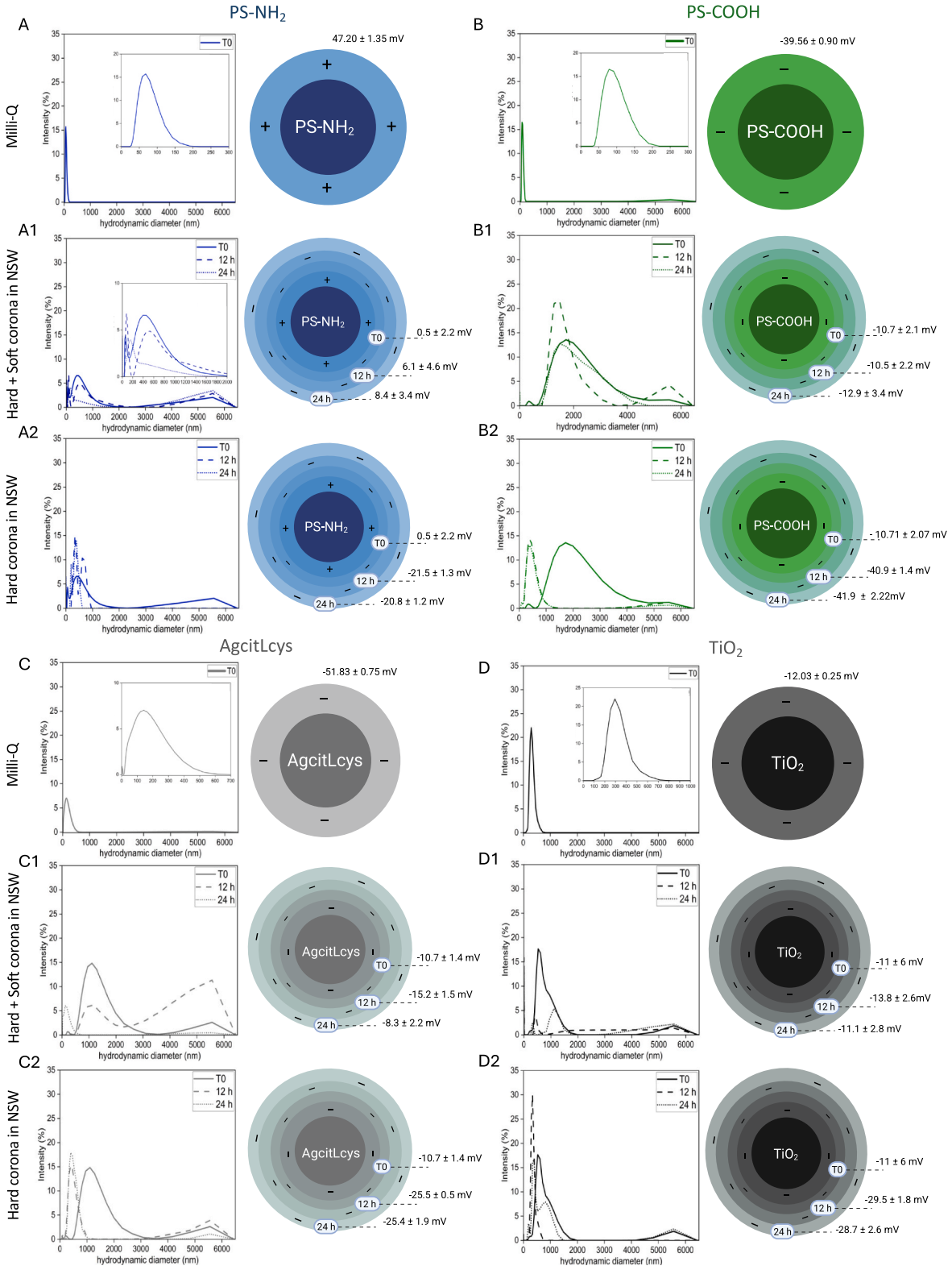

Fig. 1. Dynamic characterization of four NPs by DLS and ζP in Milli-Q (T0) and NSW suspensions, at different time points (T0, 12 h, 24 h). Charts A, B, C, and D display the intrinsic dimensions of the NPs in Milli-Q. Charts A1, B1, C1, and D1 illustrate the NPs after 24 h of incubation in the NSW. Charts A2, B2, C2, and D2 show the NPs following two PBS washes, retaining only the hard corona.

environmental fate and biological interactions (Corsi et al., 2020; Wheeler et al., 2021). In this study, DLS, ζP and TEM analysis (Figs. 1–2) revealed that NPs suspensions of all tested NP (PS-NH_2, PS-COOH, AgcitLcys, TiO_2) possessed very different D_H, surface charge and shape in Milli-Q and NSW. It should be noted that higher NP concentrations were required for DLS measurements than those used in the biological exposure experiments, as environmentally realistic concentrations would yield scattering intensities at or below the instrument's detection threshold. In Milli-Q, all NPs showed D_H and ζP values consistent with their expected physicochemical properties. PS-NH_2 and PS-COOH (Fig. 1A-B) exhibited a D_H of 63.2 ± 2.4 nm and 81.0 ± 1.5 nm, respectively, with strongly positive (+47.2 ± 1.7 mV) and negative (-39.6 ± 0.9 mV) ζP values. These ζP values, exceeding the ±30 mV threshold commonly associated with colloidal stability, indicate electrostatically stable suspensions, in agreement with established criteria for colloidal systems (Bhattacharjee, 2016). This interpretation was further supported by TEM images (Fig. 2A-B), which revealed homogeneous dispersions and well-defined spherical morphology, indicative of high colloidal stability in the absence of aggregation. AgcitLcys NPs (Fig. 1C) displayed a smaller D_H size (56.8 ± 3.1 nm) and a highly negative ζP value (-51.8 ± 0.8 mV). In contrast, TiO_2 exhibited a much larger D_H (395.2 ± 15.7 nm) and a moderately negative ζP (-12.0 ± 0.3 mV), consistent with a tendency to aggregate even at low ionic strength. TEM observations (Fig. 2C-D) further supported these findings, showing well-dispersed AgcitLcys particles and extensive aggregation of TiO_2 NPs, in agreement with previous studies (Brunelli et al., 2013; Lowry et al., 2012).

When incubated in NSW, marked changes were observed for all NPs, consistent with rapid interfacial interactions involving the adsorption of salts and biomolecules (Fig. 2.A1-D1). The intensity-weighted DLS distributions revealed the presence of multiple particle populations for all NPs, with greater heterogeneity observed for PS-COOH and AgcitLcys at 12 h (Fig. 1.B1- C1). This pattern suggests that particles may be distributed across different states of interaction with NSW components, with smaller species being transiently stabilized and larger aggregates likely associated with ionic screening or incomplete surface coverage (Baalousha et al., 2022; Grassi et al., 2019). PS-NH_2 NPs showed an initial increase in D_H (169.8 ± 7.2 nm at T_0), accompanied by a strong reduction in ζP to near-neutral values (+0.5 ± 0.6 mV). This early destabilization likely resulted from the rapid adsorption of ions of opposite charge and organic ligands onto the positively charged surface. Over time, D_H progressively decreased to 90.4 ± 4.1 nm at 12 h and 40.4 ± 2.8 nm at 24 h, while ζP partially recovered to +6.1 ± 0.8 mV and +8.4 ± 1.1 mV.

Consistently, TEM images (Fig. 2.A1) revealed the presence of thin organic coatings surrounding PS-NH_2 NPs, indicative of the compaction of an initially disordered corona into a more stable layer. In contrast, PS-COOH NPs underwent extensive aggregation, with the D_H of the most abundant population increasing to 1489 ± 53 nm at T_0 and 2587 ± 61 nm at 12 h, before partially decreasing to 797 ± 30 nm at 24 h (Fig. 1.B2). TEM confirmed the presence of large agglomerates (Fig. 2.B2). This behavior matches previous observations (Eliso et al., 2020; Murano et al., 2021; Grassi et al., 2019) and is consistent with strong electrostatic screening by divalent cations (Ca^{2+}, Mg^{2+}) promoting bridging between carboxyl groups (Tallec et al., 2019). AgcitLcys NPs (Fig. 1.C2) displayed instead pronounced fluctuations in both D_H and ζP, indicating unstable and competitive interactions with NSW. D_H varied markedly (1045 ± 43 nm at T_0, 758 ± 36 nm at 12 h, 2463 ± 74 nm at 24 h), while ζP remained slightly negative and of low magnitude (-10.7 ± 0.8 mV), consistent with extensive charge masking. This dynamic pattern likely

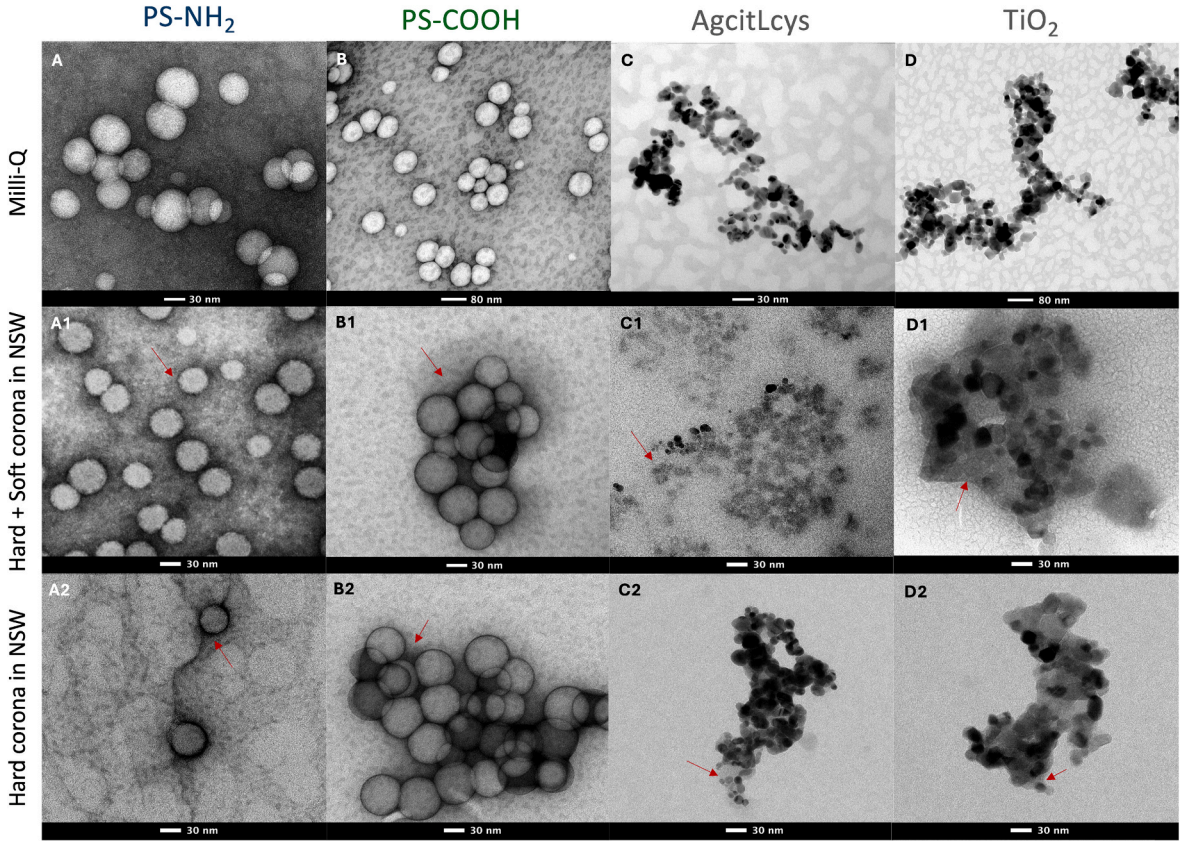

Fig. 2. Morphological and dimensional characterization of the four NP batches (PS-NH_2, PS-COOH, AgcitLcys and TiO_2) NPs using TEM. Panel A-D shows the morphology and size of NPs in Milli-Q. Panels A1-D1 display the same NP after 24 h of incubation in NSW, highlighting the formation of the eco-corona (hard + soft). Panels A2-D2 show the NPs following three PBS washes, in which only the hard corona remains after removal of the loosely bound. Arrows indicate the presence of the eco-corona where visible.

reflects alternating phases of aggregation and partial stabilization driven by high ionic strength and the adsorption of organic and inorganic species. Similar transformations were reported by Bellingeri et al. (2025), who observed a marked size increase and strong ζP reduction for AgNPcitLcys NPs in NSW, and by Wang et al. (2014), who showed that dissolved organic carbon can mitigate aggregation through the formation of stabilizing macromolecular coatings. TiO_2 NPs also exhibited strong aggregation, with D_H increasing to 821 ± 35 nm at T_0 and 1311 ± 48 nm at 12 h, remaining elevated at 1066 ± 39 nm after 24 h. Despite these size increases, moderately negative ζP values were maintained throughout incubation. This behavior is consistent with previous observations showing that TiO_2 NPs undergo hetero-aggregation with negatively charged natural colloids in saline media, forming composite aggregates stabilized by partial electrostatic compensation (Labille et al., 2015). Natural organic matter (NOM) may further modulate these interactions through surface coating or inter-particle bridging, as reported by Luo et al. (2018), with effects ranging from enhanced aggregation to partial stabilization under high ionic strength conditions. Despite the extensive aggregation, TEM observations highlighted (Fig. 2.C1-D1) the presence of a thin organic coating of NSW components also on AgcitLcys and TiO_2 NPs.

After PBS washing, which removed the soft corona, and resuspension in Milli-Q (Fig. 1.A2; B2; C2; D2), NPs coated by the sole hard eco-corona firmly bound to the surface were characterized. This was evidenced by the non-reversible changes in hydrodynamic diameter and ζP across all samples. PS-NH_2 NPs initially measured 170 ± 4.5 nm at T_0 (ζP: +0.5 ± 2.2 mV), 1215 ± 419.5 nm but after 12 h incubation followed by washing, size increased to 1215 ± 419 nm and surface charge inverted to −22 ± 1.3 mV. At 24 h, aggregation decreased slightly (859 ± 160 nm) with minimal additional changes in ζP.; PS-COOH NPs showed a similar trend. From an initial size of 1489 ± 117 nm at T_0, particles disaggregated substantially to 377 ± 17 nm at 12 h and 348 ± 21 nm at 24 h post-wash, likely reflecting soft corona removal. Meanwhile, ζP values became more negative, shifting from -10.7 ± 2.1 mV to -41.9 ± 2.2 mV, indicating surface restructuring consistent with the stable binding of marine biomolecules, forming a persistent hard corona. AgcitLcys NPs, initially smaller (758 ± 43 nm), showed similar hardening dynamics, stabilizing at 648 ± 84 nm at 24 h and increasing in surface negativity (from -10.7 ± 1.4 mV to −25.4 ± 1.9 mV). These values support the development of a partially condensed, biologically modified surface layer. TiO_2 NPs remained aggregated throughout (821 ± 97 nm at T_0 to 749 ± 131 nm at 24 h) but exhibited a marked shift in ζP from −11.0 ± 6.0 mV to −28.7 ± 2.6 mV, confirming progressive stabilization and charge inversion. This transition, also visible in TEM micrographs (Fig. 2.A2-D2), confirms the persistence of a thin hard eco-corona firmly bound to the NP surface across all materials. Together, these data indicate that, despite particle-specific differences in aggregation kinetics, the formation of a hard eco-corona is a common and robust feature in marine environments. This adsorbed layer redefines the colloidal identity of NPs over time and likely plays a central role in modulating downstream biological interactions. Although eco-corona formation may initially promote aggregation and attenuate acute surface reactivity, it may also enhance NP biological identity and persistence in the biological milieu, thereby contributing to prolonged exposure and delayed biological effects.

3.2. In vivo ecotoxicological outcomes

3.2.1. Coelomocytes viability

Coelomocytes are key components of the immune system in *P. lividus*, and their viability provides a sensitive endpoint to evaluate NPs-induced cytotoxicity (Pinsino and Matranga, 2015). After 7 days of *in vivo* exposure, the viability of coelomocytes varied markedly depending on NP type (Fig. 3A). Polymeric NPs (PS-NH_2 and PS-COOH) induced modest effects, and coelomocyte viability remained at ~84% and ~93%, respectively, relative to controls (100%). In contrast, exposure to either AgcitLcys or TiO_2 NPs caused a significant reduction for both (~-34% and ~-35%, respectively) ($p = 0.020$). This cytotoxicity pattern may reflect the unique colloidal stability and eco-corona characteristics described above for these metal-based NPs. Contrarily, polymeric NPs, showing more compact and stable eco-coronas in NSW, exhibited limited surface reactivity, consistent with the absence of cytotoxic responses (see DLS data). These results align with the trends observed in *in vitro* results by Murano et al. (2021) and Marques-Santos et al. (2018). In particular, Marques-Santos et al. (2018) reported no significant effects of PS-COOH up to 25 μg mL^{-1}, whereas PS-NH_2 caused a slight but significant reduction after 4 h in CF, decreasing from 89.66 ± 0.57% (control) to 84% and 79.33% at 10 and 25 μg mL^{-1} (i.e., -5.66 and -10.33 percentage points vs their control). Murano et al. (2021) reported an ≈ -20 percentage-point reduction under their *in vitro* conditions. In our 7 day *in vivo* exposure, PS-NH_2 induced a comparable moderate reduction (to ~84% of control), despite substantial differences in exposure duration, biological matrix, and NP transformation processes. Comparable sensitivity to AgcitLcys has been reported in *P. lividus* by Gambardella et al. (2016), who observed a significant (~40%) reduction in coelomocyte viability following 24 h exposure to 10 μg L^{-1} of AgNPs. Similar reductions in coelomocyte viability induced by TiO_2 NPs have been reported by Alijagić et al. (2019) and Catalano et al. (2020), who observed comparable cytotoxic effects (~30-40% decrease) in *P. lividus* after 72 h of exposure to higher concentrations (≥100 μg mL^{-1}). These findings support the view that prolonged exposure can elicit equivalent levels of toxicity even at lower, environmentally relevant doses. These results are in line with published *in vitro* observations, where both AgcitLcys and TiO_2 NPs induced concentration-dependent reductions in coelomocyte viability. This convergence across experimental conditions, despite the differences in exposure matrix (NSW *vs* CF), exposure time, and particle transformation dynamics, suggests a consistent biological sensitivity of sea urchin cell viability to metal-based NPs (Romano et al., 2026). It also underscores how the interaction of NPs with distinct biological fluids may modulate, but not override, their intrinsic toxicity. *In vivo*, the formation of eco-coronas in NSW appears to attenuate acute surface reactivity, yet still permits cellular effects over prolonged exposures; in the case of AgcitLcys, such effects may plausibly arise from multiple, non-mutually exclusive mechanisms, including a contribution of metal species released during exposure as well as coating/corona-mediated interactions that may favour membrane adhesion and/or cellular internalization (Bellingeri et al., 2022, 2024). In contrast, *in vitro* exposure in CF involves direct contact with immune proteins, likely amplifying early stress responses (Romano et al., 2026).

3.2.2. Red cell count

Red cells represent a specialized subpopulation of coelomocytes involved in the immune defense of *P. lividus* and are considered sensitive indicators of stress and immune activation (Pinsino and Matranga, 2015). In individuals exposed to NSW only, red cells accounted for ~7% of the total coelomocytes population, reflecting baseline physiological conditions (Liu et al., 2022). Polymeric NPs induced moderate but significant increases in their number (~10% and ~11%; $p < 0.01$), indicating mild immune activation without overt cytotoxicity. This is in line with previous observations and reflects a controlled physiological response rather than a pathological effect (Grassi et al., 2019). Metal-based NPs elicited stronger increases (~13% and ~15%; $p \leq 0.05$) (Fig. 3B). These results are consistent with previous findings on *P. lividus* exposed to different classes of contaminants, which similarly reported an increase in red cell abundance as a hallmark of immune activation. Stabili and Pagliara (2015) observed that exposure to the pesticide lindane caused a relative rise in red spherule cells despite an overall decrease in total coelomocyte count, suggesting a selective activation or resilience of this cell type under chemical stress. Likewise, Milito et al. (2020) found that long-term exposure to polluted marine sediments, rich in metals and aromatic hydrocarbons, induced a sustained increase in red amoebocytes, correlated with enhanced

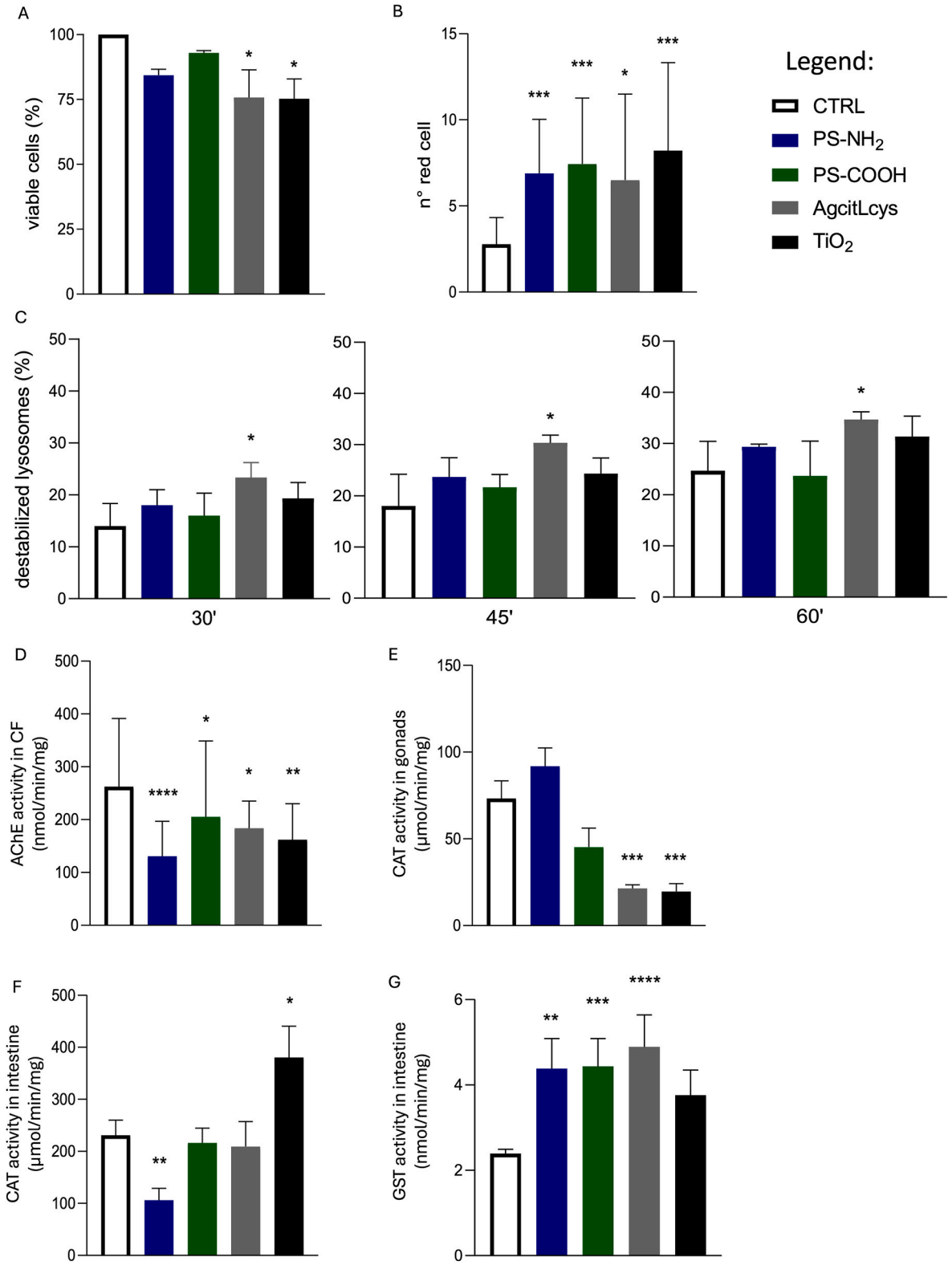

Fig. 3. Cellular and enzymatic biomarkers in *P. lividus* after *in vivo* exposure to NPs. Evaluated endpoints included cell viability, red cells count, lysosomal stability, and enzyme activities in different tissues. A) Percentage of viable *P. lividus* coelomocytes after 7 days of *in vivo* exposure B) Number red cells per 100 coelomocytes C) Percentage of lysosomal membrane destabilization D) Acetylcholinesterase (AChE) activity in coelomic fluid, expressed as µmol of substrate hydrolyzed min^{-1} mg^{-1} protein (E) Catalase (CAT) activity in gonads, and (F) CAT activity in intestine, both expressed as µmol H_2O_2 decomposed min^{-1} mg^{-1} protein.G) Glutathione S-transferase (GST) activity in intestine, expressed as nmol of conjugated product min^{-1} mg^{-1} protein. Asterisks indicate significance levels relative to control: $p < 0.05$; $^{**}p < 0.01$; $^{***}p < 0.001$; $^{****}p < 0.0001$. (For interpretation of the references to colour in this figure legend, the reader is referred to the Web version of this article.)

antioxidant capacity and contaminant bioaccumulation. In both cases, the elevation in red cells was interpreted as part of an adaptive immune and antioxidant response to persistent environmental stressors. The similar trend observed in our study reinforces the view that red spherule cells act as sensitive and early indicators of stress, responding consistently to a wide range of xenobiotic challenges, from organic pollutants to metal-based NPs.

3.2.3. Lysosomal membrane stability

LMS is a well-established biomarker of cellular stress in echinoderm coelomocytes, as the loss of lysosomal integrity represents one of the earliest signs of cytotoxicity and immune activation (Pinsino and Alijagic, 2019). The NRRT assay evaluates LMS by measuring the retention time, within the lysosomes, of the dye neutral red. Polymeric NPs (PS-NH_2 and PS-COOH) induced only mild or moderate effects on coelomocyte LMS. After 7 days of *in vivo* exposure, PS-NH_2 NPs exposure caused a slight but non-significant reduction in neutral red retention time (Fig. 3C), whereas PS-COOH NPs caused negligible variation compared to controls. In contrast, AgcitLcys NPs exposure induced the most pronounced destabilization of lysosomal membranes, with NRRT values increasing by approximately 45% at 30 min, 68% at 45 min, and 70% at 60 min relative to controls. TiO_2 NPs also promoted a measurable, though less intense, destabilization (25%, 35%, and 40%, respectively) (Fig. 3C). Overall, these LMS patterns mirror the cytotoxicity trends described above and fit well within the broader literature. The observed lysosomal membranes destabilization indicates the involvement of the lysosomal compartment in coelomocyte responses to NPs. In this context, eco-corona formation may influence not only nanoparticle uptake and cell interaction, but also their subsequent intracellular processing within the lysosomal compartment (Murano et al., 2021). The modest destabilization induced by PS-NH_2 NPs and the negligible impact of PS-COOH NPs are in agreement with *in vitro* studies in *P. lividus* coelomocytes, where PS-NH_2 can induce lysosomal destabilization while PS-COOH generally does not, even at higher concentrations and shorter exposure times (Murano et al., 2021; Marques-Santos et al., 2018). In the present study, the attenuated response likely reflects longer exposure and eco-corona formation in both seawater and coelomic fluid, which shield reactive sites and dampen acute membrane damage. Comparable lysosomal impairment was recently reported in *M. galloprovincialis* hemocytes, where exposure to AgNPcitLcys NPs triggered oxidative stress and superoxide anion generation, mechanisms known to disrupt proton gradients and compromise lysosomal integrity (Bellingeri et al., 2025). These findings are consistent with those of Alijagić et al. (2019, 2020), who reported LMS destabilization in *P. lividus* coelomocytes after 72 h at 100 μg mL^{-1}, and of Canesi et al. (2010), who observed similar effects in mussel hemocytes after 24 h at 10 μg mL^{-1}, although the NPs investigated in those studies differed in surface functionalization. The comparable destabilization observed after our 7-day exposure, despite the lower concentrations used, indicates that prolonged *in vivo* contact can induce lysosomal impairment even at environmentally relevant doses. Although differences in NP surface chemistry should be taken into account, the consistent occurrence of LMS destabilization across species and exposure conditions points to NP biomolecule interactions at the nano-bio interface as a key determinant of toxicity.

3.2.4. Acetilcolinesterase activity

AChE is a key enzyme in cholinergic neurotransmission and its activity is widely recognized as a sensitive biomarker of neurotoxicity in marine invertebrates. In *P. lividus*, its occurrence and catalytic activity in the coelomic fluid were first characterized by Cunha et al. (2005), who demonstrated that AChE and GST are enzymes constitutively expressed in this matrix and respond sensitively to xenobiotic exposure. All NP-exposed groups exhibited decreased AChE activity compared to controls, with the strongest inhibition induced by PS-NH_2 NPs, showing an approximately 50% reduction compared to controls ($p < 0.0001$), followed by TiO_2 (39%, $p = 0.0026$), AgcitLcys (31% $p = 0.2872$) and PS–COOH (22% $p = 0.0128$) (Fig. 3D). The pronounced inhibition associated with PS-NH_2 NPs is consistent with their residual cationic reactivity and potential to interact directly with cholinergic enzymes or their associated proteins in the coelomic fluid. Our results are strongly supported by Varò et al. (2019), who reported that short- and long-term exposure of *Artemia franciscana* to PS-NH_2 NPs (0.1–10 μg mL^{-1}) induced a decrease in AChE activity together with oxidative stress and developmental/physiological alterations, supporting a mechanistic link between nanoplastic exposure, redox imbalance and neurotoxic effects. Other studies on the ascidian *Ciona robusta* (Eliso et al., 2020) also support this interpretation, showing that embryos are markedly more sensitive to PS-NH_2 NPs, which induced dose-dependent developmental impairment between 2.5 and 15 μg mL^{-1}, while PS-COOH NPs do not cause any relevant developmental effects up to 100 μg mL^{-1}. A significant inhibition of AChE activity was observed in *P. lividus* exposed to AgcitLcys NPs, confirming that nanosilver can impair cholinergic function even at environmentally relevant concentrations based on predicted environmental values (Gottschalk et al., 2009; Keller et al., 2024). This trend is consistent with Zhang et al. (2018), who reported a significant inhibition of AChE activity in the marine clam *Ruditapes philippinarum* following AgNP exposure. In their study, the addition of humic acids, although reducing the overall Ag body burden, did not alleviate the neurotoxic effects, suggesting that nanosilver toxicity is primarily associated with its intrinsic physicochemical properties and ion release dynamics. TiO_2 NPs also induced a significant inhibition of AChE activity, consistent with the patterns observed for the other biomarkers investigated. This response aligns with what observed by Gambardella et al. (2013), who reported significant alterations in AChE activity in *P. lividus* larvae derived from sperm exposed to TiO_2 and Co NPs, regardless of exposure concentration. These authors suggested that NP size and morphology, rather than dose alone, play a crucial role in determining neurotoxic outcomes. Similarly, Falugi et al. (2012) observed strong inhibition of cholinesterase activity and morphological alterations in sea urchin *P. lividus* immune cells following exposure to metal oxide NPs (Fe_3O_4, CeO_2, SnO_2), supporting the notion that particle-cell interactions and redox imbalance underlie TiO_2 induced neurotoxicity in *P. lividus*.

3.2.5. Catalase activity

CAT is a fundamental antioxidant enzyme that decomposes hydrogen peroxide (H_2O_2) into water and oxygen. CAT activity exhibited distinct tissue-specific patterns in *P. lividus* following NP exposure, a trend consistent with the tissue-dependent antioxidant modulation described for other sea urchins as *Echinometra lucunter* upon aerial exposure (Pereira et al., 2025). In the gonads, CAT activity decreased in all treatments except that with PS-NH_2 NPs, which caused a slight, non-significant increase. The reduction was significant only in the case of AgcitLcys (71%, $p = 0.0009$) and TiO_2 NPs (73%, $p = 0.0004$) (Fig. 3E). A similar inhibition of CAT activity has been reported in the marine mussel *Mytilus galloprovincialis* exposed to the Ag product nanArgen™, where Ag^+ ions were shown to interact with thiol (-SH) groups of antioxidant enzymes, leading to their inactivation and the onset of oxidative stress (Ale et al., 2019). It is therefore reasonable to hypothesize that a similar process occurs in the gonads of *P. lividus* exposed to AgcitLcys. However, the antioxidant capacity of *P. lividus* gonadal tissues is not solely dependent on enzymatic defenses. Echinoderms possess additional thiol-based systems, in particular ovothiols, sulfur-containing histidine derivatives that are highly abundant in sea urchin gametes and act as potent non-enzymatic ROS scavengers (Castellano et al., 2016). Recent studies again on marine mussel *M. galloprovincialis* exposed to microplastics have shown that ovothiol levels and metabolism are actively modulated under conditions of oxidative stress, suggesting that similar compensatory mechanisms may operate in *P. lividus* gonads when CAT activity is reduced (Murano et al., 2023). In this context, it should be noted that the sex of the exposed sea

urchins was not determined. Since sex-related differences in gonadal and biochemical responses, including catalase activity, have been reported in *P. lividus* (Marčeta et al., 2020; Asnicar et al., 2024), possible sex-related variability should be considered when interpreting gonadal CAT responses. Nevertheless, the marked and statistically significant CAT inhibition observed after AgcitLcys and TiO_2 exposure supports an NP-specific effect despite this source of biological variability. In contrast, we observed an opposite pattern the intestine (Fig. 3F), where PS-NH_2 NPs significantly reduced CAT activity (55%, $p = 0.0038$), a response consistent with the capacity of these NPs to interact strongly with intestinal membranes and mucosal proteins. This mechanism, which may contribute to redox perturbation and suppression of antioxidant enzyme activity, has been well documented in bivalves exposed to cationic PS NPs, indicating that similar surface charge-dependent interactions may occur in *P. lividus* intestinal tissues (Canesi et al., 2017). Conversely, TiO_2 NPs induced a significant up-regulation of CAT (62%, $p = 0.0480$), aligning with previous findings showing that TiO_2 exposure activates antioxidant pathways and MAPK signaling in *P. lividus* (Alijagic et al., 2019; 2020). PS-COOH and AgcitLcys NPs did not induce significant changes in intestinal CAT activity, suggesting greater redox resilience in digestive tissues relative to reproductive ones. Taken together, these findings indicate that gonadal tissues are particularly vulnerable to redox imbalance, displaying a limited ability to compensate for redox perturbations once enzymatic defenses are impaired. The marked CAT inhibition observed upon metallic NP exposure suggests an altered redox balance in the gonads that may compromise reproductive redox homeostasis, with potential implications for gamete quality, fertilization success, and long-term population fitness. This sensitivity is consistent with previous findings showing that gonadal tissues of sea urchins exhibit reduced antioxidant plasticity and are among the first organs to reflect stress-induced metabolic disruption (Marčeta et al., 2020; Fouzai et al., 2023). In contrast, the intestine appears to function as a highly adaptive redox-responsive barrier, capable of modulating its antioxidant capacity in accordance with the physicochemical properties of the NPs and the redox burden imposed. The opposite regulatory trends observed in CAT inhibition under PS-NH_2 exposure versus activation under TiO_2, highlight the intestine's functional flexibility, likely linked to its direct interface with ingested or absorbed particles and its central role in metabolic processing and detoxification. In the intestine, GST and CAT responses point to complementary but NP-specific antioxidant and detoxification strategies, whereas gonadal CAT responses highlight the distinct vulnerability of reproductive tissues to redox imbalance.

3.2.6. Glutathione S-transferase activity

GST activity is a key biomarker of environmental stress in sea urchins, with increased activity reported in populations from metal- and organic-contaminated coastal areas (Cunha et al., 2005) and in individuals exposed to microplastics and associated chemicals (Digka et al., 2023). Such findings indicate that GST plays a central role in the detoxification and antioxidant defense system of *P. lividus*, particularly in digestive tissues directly interacting with environmental stressors. We found that GST activity was significantly higher in the intestine of *P. lividus* following NPs exposure, with the stronger effect (over 100% compared to controls, $p < 0.0001$) induced by AgcitLcys NPs, followed by PS-COOH (91%, $p = 0.0007$) and PS-NH_2 (85%, $p = 0.0012$), which displayed comparable activities. TiO_2 also promoted an increase, although not statistically significant (57%, $p = 0.0647$) (Fig. 3G). This consistent increase in GST activity upon NPs exposure reflects an enhanced detoxification demand and activation of antioxidant defenses in the intestine, confirming its central role as the primary interface for ingested or absorbed particles. In line with previous findings for *P. lividus*, exposure to TiO_2 NPs has been shown to activate redox-responsive and antioxidant pathways, including ROS related glutathione metabolism and the pentose phosphate pathway (Alijagic et al., 2019, 2020), supporting the enzymatic activation observed in this study. The response observed for PS-COOH NPs aligns with findings in bivalves where enhanced antioxidant enzyme activity through interactions with the intestinal mucosa have been described (Canesi et al., 2017). Moreover, the activation detected for PS-COOH and PS-NH_2 in this study may be influenced by protein corona formation and seawater-driven aggregation, which can enhance particle association with the mucosal barrier (Grassi et al., 2019). The higher GST activity observed upon AgcitLcys NPs exposure is consistent with findings in the mussel *M. galloprovincialis* exposed to the AgNP-enabled product nanArgen™ (1 and 10 μg L^{-1} for 96 h), where oxidative stress induced phase II detoxification responses, including enhanced GST activity (Ale et al., 2019). Overall, these results confirm that GST activity in the intestine of *P. lividus* responds sensitively to different NP types, reflecting a general activation of detoxification and antioxidant pathways rather than direct evidence of oxidative stress.

4. Conclusion

Our study represents the first *in vivo* investigation linking time-dependent physicochemical transformations of four types of NPs in NSW to biological responses in the sea urchin *P. lividus* exposed at environmentally relevant/predicted concentrations. Overall findings demonstrate that NPs behavior in NSW is highly dynamic: all tested NPs exhibited significant changes in size, surface charge, and aggregation state over time, reflecting complex interactions with salts and dissolved organic matter present in NSW. These transformations, associated with the progressive formation of an eco-corona, modulate the biological response of the particles by influencing their colloidal stability and interactions with the sea urchin. Different NP types exhibited distinct behaviors and biological outcomes. Polymeric NPs elicited limited physiological responses: PS-COOH was the least reactive, showing negligible effects on coelomocyte viability, LMS, AChE and CAT activity, while inducing only GST activation in intestinal tissue. Instead, despite exhibiting colloidal stability in NSW, PS-NH_2 NPs retained moderate surface reactivity, as reflected by slight inhibition of AChE and intestinal CAT activity, increased GST activity, and mild immune activation (i.e., elevated red cell counts), without significantly impacting coelomocyte viability or LMS. These findings suggest that although reorganization of the NP interface, via adsorption of marine biomolecules, likely dampens acute interactions, the residual positive charge on PS-NH_2 NPs allows for continued interaction with cellular membranes and functional proteins. In contrast, metal-based NPs elicited more pronounced effects. AgcitLcys NPs exposure resulted in a marked reduction of coelomocyte viability, significant lysosomal destabilization, strong inhibition of CAT activity in gonads, and upregulation of GST in the intestine. TiO_2 induced comparable toxicity: reduced cellular viability, compromised LMS, elevated red cell counts, AChE and CAT inhibition in gonadal tissues, and a significant induction of intestinal CAT activity, indicative of an adaptive oxidative response. These effects were plausibly driven by their higher colloidal instability, tendency toward heterogeneous aggregation, and intrinsic properties such as ion release and redox activity. Overall, our findings support the notion that NPs ecotoxicity is modulated by their dynamic behavior in marine waters, which redefines their biological identity and modulates bioavailability. The multiparametric approach adopted here enabled a nuanced understanding of the link between colloidal dynamics and biological responses, shedding light on the mechanisms underlying nanoparticle-organism interactions. Importantly, these results indicate that Marine Environmental Risk Assessment of nanomaterials should not rely solely on the pristine physicochemical properties of the tested materials, but should also account for their seawater-driven transformations, including eco-corona formation, aggregation behavior, and the resulting changes in bioavailability. Integrating physicochemical characterization with ecotoxicological biomarker assessment thus emerges as a fundamental strategy for developing predictive, evidence-based tools. In this perspective, the inclusion of environmentally transformed NP identities

and tissue-specific biological responses may improve the realism and predictive power of hazard characterization, thereby supporting more robust and ecologically relevant regulatory frameworks for nanomaterial safety in marine ecosystems.

CRediT authorship contribution statement

Patrizia Romano: Writing – original draft, Methodology, Investigation, Formal analysis, Data curation. **Sofia Bichi:** Investigation, Formal analysis, Data curation. **Nour Oueslati:** Investigation, Data curation. **Eugenio Paccagnini:** Writing – review & editing, Methodology, Investigation. **Najoua Trigui El Menif:** Writing – review & editing, Supervision. **Pietro Lupetti:** Writing – review & editing, Supervision, Resources. **Iole Venditti:** Writing – review & editing, Resources. **Serena Leone:** Writing – review & editing, Supervision, Conceptualization. **Ilaria Corsi:** Writing – review & editing, Supervision, Conceptualization.

Declaration of competing interest

The authors declare that they have no known competing financial interests or personal relationships that could have appeared to influence the work reported in this paper.

Acknowledgements

P.R. has been supported by a PhD fellowship co-funded by the Stazione Zoologica Anton Dohrn and the University of Siena (PhD in Environmental, geological and polar sciences and technologies).

Data availability

The authors do not have permission to share data.

References

Aebi, H., 1984. Catalase in vitro. Method Enzymol 105, 121–126. https://doi.org/10.1016/S0076-6879(84)05016-3.

Ale, A., Liberatori, G., Vannuccini, M.L., Bergami, E., Ancora, S., Mariotti, G., Bianchi, N., Galdopórpora, J.M., Desimone, M.F., Cazenave, J., Corsi, I., 2019. Exposure to a nanosilver-enabled consumer product results in similar accumulation and toxicity of silver nanoparticles in the marine mussel *Mytilus galloprovincialis*. Aquat. Toxicol. 211, 46–56. https://doi.org/10.1016/j.aquatox.2019.03.018.

Alijagic, A., Benada, O., Kofroňová, O., Cigna, D., Pinsino, A., 2019. Sea urchin extracellular proteins design a complex protein Corona on titanium dioxide nanoparticle surface influencing immune cell behavior. Front. Immunol. 10, 2261. https://doi.org/10.3389/fimmu.2019.02261.

Alijagic, A., Gaglio, D., Napodano, E., Russo, R., Costa, C., Benada, O., Kofroňová, O., Pinsino, A., 2020. Titanium dioxide nanoparticles temporarily influence the sea urchin immunological state suppressing inflammatory-related gene transcription and boosting antioxidant metabolic activity. J. Hazard Mater. 384, 121389. https://doi.org/10.1016/j.jhazmat.2019.121389.

Al-Sid-Cheikh, M., Rowland, S.J., Stevenson, K., Rouleau, C., Henry, T.B., Thompson, R. C., 2018. Uptake, whole-body distribution, and depuration of nanoplastics by the scallop Pecten maximus at environmentally realistic concentrations. Environ. Sci. Technol. 52 (24), 14480–14486. https://doi.org/10.1021/acs.est.8b05266.

Arizza, V., Vazzana, M., Schillaci, D., Russo, D., Giaramita, F.T., Parrinello, N., 2013. Gender differences in the immune system activities of sea urchin *Paracentrotus lividus*. Comp. Biochem. Physiol. Mol. Integr. Physiol. 164 (3), 447–455. https://doi.org/10.1016/j.cbpa.2012.11.021.

Asnicar, D., Stranci, F., Monti, S., Badocco, D., Marčeta, T., Munari, M., Marin, M.G., 2024. Investigating intraspecific variability in the biological responses of sea urchins (*Paracentrotus lividus*) to seawater acidification. Environ. Sci. Pollut. Res. Int. 31 (39), 51687–51701. https://doi.org/10.1007/s11356-024-34618-7.

Baalousha, M., Sikder, M., Poulin, B.A., Tfaily, M.M., Hess, N.J., 2022. Natural organic matter composition and nanomaterial surface coating determine the nature of platinum nanomaterial-natural organic matter corona. Sci. Total Environ. 806, 150477. https://doi.org/10.1016/j.scitotenv.2021.150477.

Bhattacharjee, S., 2016. DLS and zeta potential - what they are and what they are not? J. Contr. Release: official journal of the Controlled Release Society 235, 337–351. https://doi.org/10.1016/j.jconrel.2016.06.017.

Bellingeri, A., Ale, A., Rusconi, T., Scattoni, M., Lemaire, S., Protano, G., Venditti, I., Corsi, I., 2025. Nanosilver environmental safety in marine organisms: ecotoxicological assessment of a commercial nano-enabled product vs an eco-design formulation. Toxics 13 (5), 338. https://doi.org/10.3390/toxics13050338.

Bellingeri, A., Battocchio, C., Faleri, C., Protano, G., Venditti, I., Corsi, I., 2022. Sensitivity of Hydra vulgaris to Nanosilver for environmental applications. Toxics 10 (11), 695. https://doi.org/10.3390/toxics10110695.

Bellingeri, A., Bono, N., Venditti, I., Bertelà, F., Burratti, L., Faleri, C., Protano, G., Paccagnini, E., Lupetti, P., Candiani, G., Corsi, I., 2024. Capping drives the behavior, dissolution and (eco)toxicity of silver nanoparticles towards microorganisms and mammalian cells. Environ. Sci. Nano 11 (5), 2049–2060. https://doi.org/10.1039/D4EN00063C.

Bergami, E., Pugnalini, S., Vannuccini, M.L., Manfra, L., Faleri, C., Savorelli, F., Dawson, K.A., Corsi, I., 2017. Long-term toxicity of surface-charged polystyrene nanoplastics to marine planktonic species Dunaliella tertiolecta and Artemia franciscana. Aquat. Toxicol. 189, 159–169.

Besseling, E., Redondo-Hasselerharm, P., Foekema, E.M., Koelmans, A.A., 2019. Quantifying ecological risks of aquatic micro- and nanoplastic. Crit. Rev. Environ. Sci. Technol. 49 (1), 32–80. https://doi.org/10.1080/10643389.2018.1531688.

Brunelli, A., Pojana, G., Callegaro, S., Marcomini, A., 2013. Agglomeration and sedimentation of titanium dioxide nanoparticles (n-TiO2) in synthetic and real waters. J. Nanoparticle Res. 15 (6), 1684. https://doi.org/10.1007/s11051-013-1684-4.

Canesi, L., Balbi, T., Fabbri, R., Salis, A., Damonte, G., Volland, M., Blasco, J., 2017. Biomolecular coronas in invertebrate species: implications in the environmental impact of nanoparticles. NanoImpact 8, 89–98. https://doi.org/10.1016/J.IMPACT.2017.08.001.

Canesi, L., Ciacci, C., Vallotto, D., Gallo, G., Marcomini, A., Pojana, G., 2010. In vitro effects of suspensions of selected nanoparticles (C60 fullerene, TiO2, SiO2) on *Mytilus hemocytes*. Aquat. Toxicol. 96 (2), 151–158. https://doi.org/10.1016/j.aquatox.2009.10.017.

Castellano, I., Migliaccio, O., D'Aniello, S., Merlino, A., Napolitano, A., Palumbo, A., 2016. Shedding light on ovothiol biosynthesis in marine metazoans. Sci. Rep. 6, 21506. https://doi.org/10.1038/srep21506.

Catalano, R., Labille, J., Gaglio, D., Alijagic, A., Napodano, E., Slomberg, D., Campos, A., Pinsino, A., 2020. Safety evaluation of TiO2 nanoparticle-based sunscreen UV filters on the development and the immunological State of the Sea urchin *Paracentrotus lividus*. Nanomaterials 10 (11), 2102. https://doi.org/10.3390/nano10112102.

Chatterjee, S., Lou, X.-Y., Liang, F., Yang, Y.-W., 2022. Surface-functionalized gold and silver nanoparticles for colorimetric and fluorescent sensing of metal ions and biomolecules. Coord. Chem. Rev. 459, 214461. https://doi.org/10.1016/j.ccr.2022.214461.

Cole, M., Lindeque, P., Halsband, C., Galloway, T.S., 2011. Microplastics as contaminants in the marine environment: a review. Mar. Pollut. Bull. 62 (12), 2588–2597. https://doi.org/10.1016/j.marpolbul.2011.09.025.

Corsi, I., Bergami, E., Grassi, G., 2020. Behavior and bio-interactions of anthropogenic particles in marine environment for a more realistic ecological risk assessment. Front. Environ. Sci. https://doi.org/10.3389/fenvs.2020.00060.

Cunha, I., García, L.M., Guilhermino, L., 2005. Sea-urchin (*Paracentrotus lividus*) glutathione S-transferases and cholinesterase activities as biomarkers of environmental contamination. J. Environ. Monitoring 7 (4), 288–294. https://doi.org/10.1039/B414773A.

Dedman, C.J., King, A.M., Christie-Oleza, J.A., Davies, G.-L., 2021. Environmentally relevant concentrations of titanium dioxide nanoparticles pose negligible risk to marine microbes. Environ. Sci. Nano 8 (5), 1236–1255. https://doi.org/10.1039/D0EN00883D.

Della Torre, C., Bergami, E., Salvati, A., Faleri, C., Cirino, P., Dawson, K.A., Corsi, I., 2014. Accumulation and embryotoxicity of polystyrene nanoparticles at early stage of development of Sea urchin embryos *Paracentrotus lividus*. Environ. Sci. Technol. 48 (20), 12302–12311. https://doi.org/10.1021/es502569w.

Digka, N., Patsiou, D., Kaberi, H., Krasakopoulou, E., Tsangaris, C., 2023. Microplastic ingestion and its effects on sea urchin *Paracentrotus lividus*: a field study in a coastal East Mediterranean environment. Mar. Pollut. Bull. 196, 115613. https://doi.org/10.1016/j.marpolbul.2023.115613.

Eliso, M.C., Bergami, E., Manfra, L., Spagnuolo, A., Corsi, I., 2020. Toxicity of nanoplastics during the embryogenesis of the ascidian *Ciona robusta* (Phylum Chordata). Nanotoxicology 14, 1415–1431. https://doi.org/10.1080/17435390.2020.1838650.

Ellman, G.L., Courtney, K.D., Andres, V., Featherstone, R.M., 1961. A new and rapid colorimetric determination of acetylcholinesterase activity. Biochem. Pharmacol. 7 (2), 88–95. https://doi.org/10.1016/0006-2952(61)90145-9.

Falugi, C., Aluigi, M., Chiantore, M., Privitera, D., Ramoino, P., Gatti, M.A., Fabrizi, A., Pinsino, A., Matranga, V., 2012. Toxicity of metal oxide nanoparticles in immune cells of the sea urchin. Mar. Environ. Res. 76, 114–121. https://doi.org/10.1016/j.marenvres.2011.10.003.

Fouzai, C., Trabelsi, W., Bejaoui, S., Marengo, M., Ghribi, F., Chetoui, I., Mili, S., Soudani, N., 2023. Dual oxidative stress and fatty acid profile impacts in *Paracentrotus lividus* exposed to lambda-cyhalothrin: biochemical and histopathological responses. Toxicol. Res. 39 (3), 429–441. https://doi.org/10.1007/s43188-023-00174-4.

Galletti, A., Seo, S., Joo, S.H., Su, C., Blackwelder, P., 2016. Effects of titanium dioxide nanoparticles derived from consumer products on the marine diatom *Thalassiosira pseudonana*. Environ. Sci. Pollut. Control Ser. 23 (20), 21113–21122. https://doi.org/10.1007/s11356-016-7556-6.

Gambardella, C., Aluigi, M., Ferrando, S., Gallus, L., Ramoino, P., Gatti, A., Rottigni, M., Falugi, C., 2013. Developmental abnormalities and changes in cholinesterase activity in sea urchin embryos and larvae from sperm exposed to engineered nanoparticles. Aquat. Toxicol. 130–131, 77–85. https://doi.org/10.1016/j.aquatox.2012.12.025.

Gambardella, C., Ferrando, S., Gatti, A.M., Cataldi, E., Ramoino, P., Aluigi, M.G., Faimali, M., Diaspro, A., Falugi, C., 2016. Review: morphofunctional and

biochemical markers of stress in sea urchin life stages exposed to engineered nanoparticles. Environ. Toxicol. 31 (11), 1552–1562. https://doi.org/10.1002/tox.22159.
Gottschalk, F., Sonderer, T., Scholz, R.W., Nowack, B., 2009. Modeled environmental concentrations of engineered nanomaterials (TiO_2, ZnO, Ag, CNT, fullerenes) for different regions. Environ. Sci. Technol. 43 (24), 9216–9222. https://doi.org/10.1021/es9015553.
Grassi, G., Landi, C., Torre, C.D., Bergami, E., Bini, L., Corsi, I., 2019. Proteomic profile of the hard corona of charged polystyrene nanoparticles exposed to sea urchin *Paracentrotus lividus* coelomic fluid highlights potential drivers of toxicity. Environ. Sci. Nano. https://doi.org/10.1039/c9en00824a.
Habig, W.H., Pabst, M.J., Jakoby, W.B., 1974. Glutathione S-Transferases. J. Biol. Chem. 249 (22), 7130–7139. https://doi.org/10.1016/S0021-9258(19)42083-8.
Jouyban, A., Rahimpour, E., 2020. Optical sensors based on silver nanoparticles for determination of pharmaceuticals: an overview of advances in the last decade. Talanta 217, 121071. https://doi.org/10.1016/j.talanta.2020.121071.
Keller, A.A., Zheng, Y., Praetorius, A., Quik, J.T.K., Nowack, B., 2024. Predicting environmental concentrations of nanomaterials for exposure assessment—A review. NanoImpact 33, 100496. https://doi.org/10.1016/j.impact.2024.100496.
Labille, J., Harns, C., Bottero, J.-Y., Brant, J., 2015. Heteroaggregation of titanium dioxide nanoparticles with natural clay colloids. Environ. Sci. Technol. 49 (11), 6608–6616. https://doi.org/10.1021/acs.est.5b00357.
Li, L., Stoiber, M., Wimmer, A., Xu, Z., Lindenblatt, C., Helmreich, B., Schuster, M., 2016. To what extent can full-scale wastewater treatment plant effluent influence the occurrence of silver-based nanoparticles in surface waters? Environ. Sci. Technol. 50 (12), 6327–6333. https://doi.org/10.1021/acs.est.6b00694.
Liu, S., Junaid, M., Liao, H., Liu, X., Wu, Y., Wang, J., 2022. Eco-corona formation and associated ecotoxicological impacts of nanoplastics in the environment. Sci. Total Environ. 836, 155703. https://doi.org/10.1016/j.scitotenv.2022.155703.
Lowry, G.V., Gregory, K.B., Apte, S.C., Lead, J.R., 2012. Guest comment: transformations of nanomaterials in the environment focus issue. Environ. Sci. Technol. 46 (13), 6891–6892. https://doi.org/10.1021/es3022039.
Luo, M., Huang, Y., Zhu, M., Tang, Y., Ren, T., Ren, J., Wang, H., Li, F., 2018. Properties of different natural organic matter influence the adsorption and aggregation behavior of TiO_2 nanoparticles. J. Saudi Chem. Soc. 22 (2), 146–154. https://doi.org/10.1016/j.jscs.2016.01.007.
Manzo, S., Schiavo, S., 2022. Physical and chemical threats posed by micro(nano)plastic to sea urchins. Sci. Total Environ. 808, 152105. https://doi.org/10.1016/j.scitotenv.2021.152105.
Marčeta, T., Matozzo, V., Alban, S., Badocco, D., Pastore, P., Marin, M.G., 2020. Do males and females respond differently to ocean acidification? An experimental study with the sea urchin *Paracentrotus lividus*. Environ. Sci. Pollut. Control Ser. 27 (31), 39516–39530. https://doi.org/10.1007/s11356-020-10040-7.
Marques-Santos, L.F., Grassi, G., Bergami, E., Faleri, C., Balbi, T., Salis, A., Damonte, G., Canesi, L., Corsi, I., 2018. Cationic polystyrene nanoparticle and the sea urchin immune system: Biocorona formation, cell toxicity, and multixenobiotic resistance phenotype. Nanotoxicology 12 (8), 847–867. https://doi.org/10.1080/17435390.2018.1482378.
Milito, A., Murano, C., Castellano, I., Romano, G., Palumbo, A., 2020. Antioxidant and immune response of the sea urchin Paracentrotus lividus to different re-suspension patterns of highly polluted marine sediments. Mar. Environ. Res. 160, 104978. https://doi.org/10.1016/j.marenvres.2020.104978.
Murano, C., Bergami, E., Liberatori, G., Palumbo, A., Corsi, I., 2021. Interplay between Nanoplastics and the immune System of the Mediterranean Sea urchin *Paracentrotus lividus*. Front. Mar. Sci. 8, 647394. https://doi.org/10.3389/fmars.2021.647394.
Murano, C., Palumbo, A., Leone, S., 2023. Toxicological impacts of microplastics: effects on levels of cellular thiols in *Mytilus galloprovincialis*. Environ. Toxicol. Chem. 42 (7), 1607–1613. https://doi.org/10.1002/etc.5643.
Natarajan, L., Jenifer, M.A., Mukherjee, A., 2021. Eco-corona formation on the nanomaterials in the aquatic systems lessens their toxic impact: a comprehensive review. Environ. Res. 194, 110669. https://doi.org/10.1016/j.envres.2020.110669.
Pereira, T.M., Minari, M., Carvajalino-Fernández, J.M., Moreira, D.C., Hermes-Lima, M., 2025. Redox metabolism during aerial exposure of the Sea urchin *Echinometra lucunter*: an ecophysiological perspective. Animals 15 (9), 1251. https://doi.org/10.3390/ani15091251.
Permana, R., Chakraborty, S., Valsami-Jones, E., 2025. Nanoplastics in aquatic environments: the hidden impact of aging on fate and toxicity. Environ. Chem. Ecotoxicol. 7, 429–444. https://doi.org/10.1016/j.enceco.2025.02.007.
Pinsino, A., Alijagic, A., 2019. Sea urchin *Paracentrotus lividus* immune cells in culture: formulation of the appropriate harvesting and culture media and maintenance conditions. Biology Open. https://doi.org/10.1242/bio.039289 bio.039289.
Pinsino, A., Matranga, V., 2015. Sea urchin immune cells as sentinels of environmental stress. Dev. Comp. Immunol. 49 (1), 198–205. https://doi.org/10.1016/j.dci.2014.11.013.
Pradel, A., Catrouillet, C., Gigault, J., 2023. The environmental fate of nanoplastics: what we know and what we need to know about aggregation. NanoImpact 29, 100453. https://doi.org/10.1016/j.impact.2023.100453.
Prasher, P., Sharma, M., Mudila, H., Gupta, G., Sharma, A.K., Kumar, D., Bakshi, H.A., Negi, P., Kapoor, D.N., Chellappan, D.K., Tambuwala, M.M., Dua, K., 2020. Emerging trends in clinical implications of bio-conjugated silver nanoparticles in drug delivery. Colloid Interface Sci. Commun. 35, 100244. https://doi.org/10.1016/j.colcom.2020.100244.
Prosposito, P., Burratti, L., Bellingeri, A., Protano, G., Faleri, C., Corsi, I., Battocchio, C., Iucci, G., Tortora, L., Secchi, V., Franchi, S., Venditti, I., 2019. Bifunctionalized silver nanoparticles as Hg^{2+} plasmonic sensor in water: synthesis, characterizations, and ecosafety. Nanomaterials 9 (10), 1353. https://doi.org/10.3390/nano9101353.
Romano, P., Bellingeri, A., Morelli, M., Lucignano, R., Paccagnini, E., Venditti, I., Carpentieri, A., Lupetti, P., Corsi, I., Leone, S., 2026. Linking protein Corona composition to ecotoxicological outcomes: a comparative Study of different engineered nanoparticles in Mediterranean Sea urchin *Paracentrotus lividus*. Environ. Sci. Nano. https://doi.org/10.1039/D5EN00836K.
Smith, L.C., Hawley, T.S., Henson, J.H., Majeske, A.J., Oren, M., Rosental, B., 2019. Methods for collection, handling, and analysis of sea urchin coelomocytes. Methods Cell Biol. 150, 357–389. https://doi.org/10.1016/bs.mcb.2018.11.009. Elsevier.
Stabili, L., Pagliara, P., 2015. The sea urchin *Paracentrotus lividus* immunological response to chemical pollution exposure: the case of lindane. Chemosphere 134, 60–66. https://doi.org/10.1016/j.chemosphere.2015.04.006.
Strober, W., 2015. Trypan blue exclusion Test of cell viability. Curr. Protoc. Im. 111 (1). https://doi.org/10.1002/0471142735.ima03bs111.
Tallec, K., Blard, O., González-Fernández, C., Brotons, G., Berchel, M., Soudant, P., Huvet, A., Paul-Pont, I., 2019. Surface functionalization determines behavior of nanoplastic solutions in model aquatic environments. Chemosphere 225, 639–646. https://doi.org/10.1016/j.chemosphere.2019.03.077.
Tovar-Sánchez, A., Sánchez-Quiles, D., Basterretxea, G., Benedé, J.L., Chisvert, A., Salvador, A., Moreno-Garrido, I., Blasco, J., 2013. Sunscreen products as emerging pollutants to coastal waters. PLoS One 8 (6), e65451. https://doi.org/10.1371/journal.pone.0065451.
Turan, N.B., Erkan, H.S., Engin, G.O., Bilgili, M.S., 2019. Nanoparticles in the aquatic environment: usage, properties, transformation and toxicity-A review. Process Saf. Environ. Prot. 130, 238–249. https://doi.org/10.1016/j.psep.2019.08.014.
Varó, I., Perini, A., Torreblanca, A., Garcia, Y., Bergami, E., Vannuccini, M., Corsi, I., 2019. Time-dependent effects of polystyrene nanoparticles in brine shrimp *Artemia franciscana* at physiological, biochemical and molecular levels. Sci. Total Environ. 675, 570–580. https://doi.org/10.1016/j.scitotenv.2019.04.157.
Wang, H., Burgess, R.M., Cantwell, M.G., Portis, L.M., Perron, M.M., Wu, F., Ho, K.T., 2014. Stability and aggregation of silver and titanium dioxide nanoparticles in seawater: role of salinity and dissolved organic carbon. Environ. Toxicol. Chem. 33 (5), 1023–1029. https://doi.org/10.1002/etc.2529.
Wheeler, K.E., Chetwynd, A.J., Fahy, K.M., Hong, B.S., Tochihuitl, J.A., Foster, L.A., Lynch, I., 2021. Environmental dimensions of the protein corona. Nat. Nanotechnol. 16 (6), 617–629. https://doi.org/10.1038/s41565-021-00924-1.
Yang, H., Chen, Z., Kong, L., Xing, H., Yang, Q., Wu, J., 2025. A review of eco-corona Formation on Micro/Nanoplastics and its effects on stability, bioavailability, and toxicity. Water 17 (8), 1124. https://doi.org/10.3390/w17081124.
Zhang, T., Pan, J., Hunt, D., Chen, M., Wang, B., 2018. Organic matter modifies biochemical but not most behavioral responses of the clam *Ruditapes philippinarum* to nanosilver exposure. Mar. Environ. Res. 133, 105–113. https://doi.org/10.1016/j.marenvres.2017.10.016.
Zheng, R., Li, L., Wu, Z., Xu, A., Xu, H., Hao, Z., Yu, S., Cai, Y., Liu, J., 2025. Distribution and source of titanium dioxide nanoparticles in seawater and sediment from Jiaozhou Bay, China. J. Hazard Mater. 483, 136576. https://doi.org/10.1016/j.jhazmat.2024.136576.